Analysis of Microstructural Changes Induced by Linear Friction Welding in a Nickel-Base Superalloy

O.T. OLA, O.A. OJO, P. WANJARA, and M.C. CHATURVEDI

A detailed microstructural analysis was performed on a difficult-to-weld nickel-base superalloy, IN 738, subjected to linear friction welding and Gleeble thermomechanical simulation, to understand the microstructural changes induced in the material. Correlations between the microstructures of the welded and simulated materials revealed that, in contrast to a general assumption of linear friction welding being an exclusively solid-state joining process, intergranular liquation, caused by nonequilibrium phase reaction(s), occurred during joining. However, despite a significant occurrence of liquation in the alloy, no heat-affected zone (HAZ) cracking was observed. The study showed that the manufacturing of crack-free welds by linear friction welding is not due to preclusion of grain boundary liquation, as has been commonly assumed and reported. Instead, resistance to cracking can be related to the counter-crack-formation effect of the imposed compressive stress during linear friction welding and strain-induced rapid solidification. Moreover, adequate understanding of the microstructure of the joint requires proper consideration of the concepts of nonequilibrium liquation reaction and strain-induced rapid solidification, which are carefully elucidated in this work.

DOI: 10.1007/s11661-011-0774-0

I. INTRODUCTION

INCONEL 738 is a γ' strengthened nickel-base superalloy used in the production of hot-section components in aero and land-based gas turbine applications due to its excellent high-temperature strength and remarkable corrosion resistance. Fabrication and repair of service-damaged turbine components often involve various joining methods. Welding has proven to be an economical way of fabricating components and repairing turbine parts. Unfortunately, IN 738, like other precipitation-hardened nickel-base superalloys that contain a substantial amount of Al and Ti, is very difficult to weld due to its high susceptibility to heat-affected zone (HAZ) cracking during conventional fusion welding processes and strain age cracking during postweld heat treatment.[1–3] The cause of this cracking, which is usually intergranular in nature, was attributed to the liquation of various phases in the alloy, subsequent wetting of the grain boundaries by the liquid, and decohesion along one of the solid-liquid interfaces due to on-cooling tensile stresses.[2–4] In order to avoid liquation and liquation cracking in superalloys, the state-of-the-art trend in joining difficult-to-weld structural materials involves the use of solid-state joining techniques. Friction welding is regarded as a solid-state joining process that has great potential in the aerospace industry for the joining of superalloys, especially for the fabrication of blade-disk assemblies and the repair of aero-engine components.[5–8] The process has produced successful joints in some structural alloys, and current research efforts are now being directed toward its application for the fabrication and repair of turbine components made of nickel-base superalloys. This present work was initiated in order to investigate the weldability of the difficult-to-weld IN 738 superalloy by linear friction welding, which is a variant of the friction welding processes, and to analyze the microstructural changes induced in the alloy by the welding process. The results are presented and discussed in this article.

O.T. OLA, Doctoral Student, O.A. OJO, Associate Professor, and M.C. CHATURVEDI, Distinguished Professor Emeritus, are with Department of Mechanical and Manufacturing Engineering, University of Manitoba, Winnipeg, MB R3T 5V6, Canada. Contact e-mail: ojo@cc.umanitoba.ca P. WANJARA, Group Leader, is with the National Research Council Canada, Institute for Aerospace Research, Aerospace Manufacturing Technology Centre, Montréal, QC H3T 2B2, Canada.

Manuscript submitted November 24, 2010.
Article published online August 16, 2011

II. EXPERIMENTAL

Cast IN 738 with a nominal composition of (wt pct) 0.11C, 15.84Cr, 8.5Co, 2.48W, 1.88Mo, 0.92Nb, 0.07Fe, 3.46Al, 3.47Ti, 1.69Ta, 0.04Zr, 0.010B, and balance nickel was received in the form of plates having dimensions of 240 mm × 60 mm × 15 mm. Welding test coupons of dimensions 12.8 mm × 11.1 mm × 17.7 mm were machined from these plates and were given the standard solution heat treatment (SHT) at 1393 K (1120 °C) for 2 hours, followed by air cooling. Linear friction welding of the specimens was performed by using a Linear Friction Welding Process Development System at the Aerospace Manufacturing Technology Centre of the Institute for Aerospace Research, National Research Council of Canada. The frequency and amplitude of oscillation during welding were 100 Hz and 2 mm,

respectively. The forging phase of the process was performed under a pressure of 90 MPa. The axial shortening, after a total welding time of 21.6 seconds, was about 1.63 mm. In order to study and decouple the effect of the nonequilibrium thermal cycle and imposed compressive stress during joining, physical simulation of the linear friction welding process was performed by using the Gleeble 1500-D thermomechanical simulation system (Dynamic System Inc., Poestenkill, NY). The Gleeble simulations were performed at a fast heating rate of 150 °C/s to temperatures ranging from 1373 K to 1523 K (1100 °C to 1250 °C) for different holding times, followed by air cooling. Specimens simulated to study the effect of thermal cycle alone, without imposed stress, were heated to the peak temperatures and held for specific holding times ranging from 0.5 to 20.5 seconds before air cooling. Specimens used to study the coupled effect of thermal cycle and imposed compressive stresses were heated to the peak temperatures, while the holding times and the percent length reductions at the peak temperatures were varied. Welded and Gleeble-simulated specimens were sectioned, prepared by standard metallographic techniques for microstructural examination, and etched electrolytically in 12 mL H_3PO_4 + 40 mL HNO_3 + 48 mL H_2SO_4 solution at 6 V for 5 seconds. Microstructures of the welded and Gleeble-simulated specimens were examined and analyzed by a Zeiss Axiovert 25 inverted reflected-light optical microscope (Carl Zeiss, Jena, Germany) equipped with a Clemex vision 3.0 image analyzer (Clemex Technologies Inc., Longueuil, Canada) and a JEOL* JSM 5900 scanning electron microscope (SEM) equipped with an Oxford (Oxford Instruments, Oxfordshire, UK) ultrathin window energy-dispersive spectrometer and Inca analyzing software. The character and distribution of grain boundaries across the weld joint were examined by carrying out electron backscatter diffraction (EBSD) based orientation imaging microscopy (OIM)** scans, with the OIM equipment attached to the JEOL JSM-5900 SEM. Special grain boundaries ($3 \le \Sigma \le 29$) were characterized based on the coincident site lattice model. The microhardness profile across the weld was determined by using a Buehler microhardness tester with a load of 300 g.

*JEOL is a trademark of Japan Electron Optics Ltd., Tokyo.

**OIM is a trademark of TexSEM Laboratories, Inc., Provo, UT.

III. RESULTS AND DISCUSSION

A. *Microstructure of the Preweld SHT Material*

An SEM micrograph of preweld SHT material is presented in Figure 1, showing a bimodal distribution of the strengthening γ' precipitates consisting of regular coarse primary γ' precipitates with sizes ranging from about 0.4 to 0.8 μm and fine spherical secondary γ' precipitates about 0.1-μm diameter. The solidification products that formed during casting,[2,3] namely, MC carbides and γ-γ' eutectic, were found to have persisted in the SHT material. Figure 1 shows MC carbides and γ-γ' eutectic, with the inset showing both the primary and secondary γ' precipitates. This type of constituents' distribution in SHT IN 738 was also observed by other researchers.[4] Significant changes in this preweld microstructure were found to occur during linear friction welding, which will be discussed in Section III–B.

B. *General Microstructure of the Welded Specimen*

Microscopic examination of linear friction welded IN 738 showed a sound and crack-free joint, as illustrated by the SEM micrograph presented in Figure 2. An overview of the welded joint revealed three different microstructural regions, which are illustrated in the optical micrograph of Figure 3. The weld zone (region 1), which formed at the interface between the two work pieces and extended to about 300 μm into the material

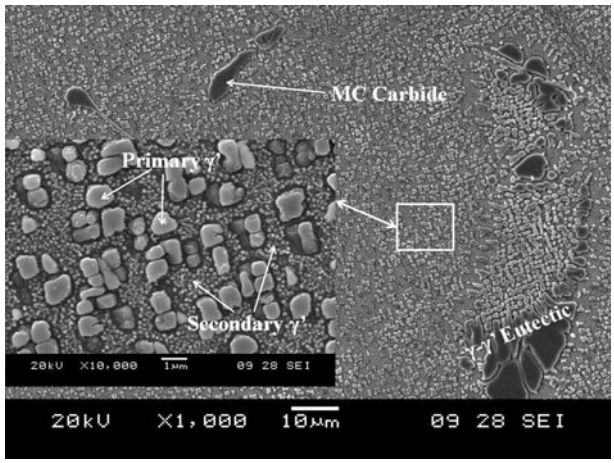

Fig. 1—SEM micrograph of solution-heat-treated IN 738 showing primary and secondary γ' precipitates, MC carbides, and γ-γ' eutectic.

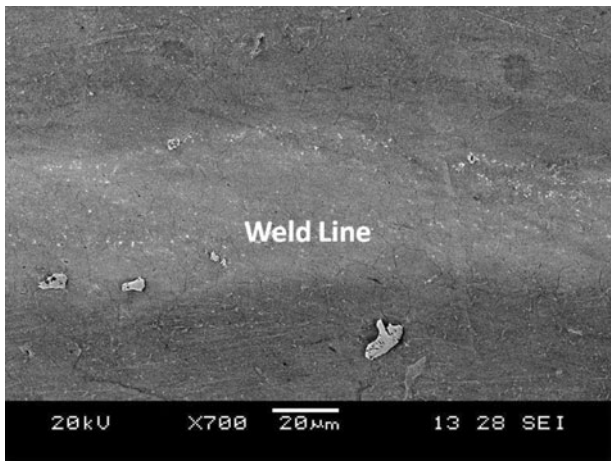

Fig. 2—SEM micrographs showing a crack-free linear friction joint in IN 738.

on either side of the joint, showed microstructural characteristics considerably different from that of the SHT specimen (Figure 1) due to the thermomechanical processing that occurred during linear friction welding. SEM analysis of this region (Figure 2) revealed that γ' precipitates, including γ-γ' eutectic, completely dissolved during linear friction welding, while MC carbides survived to the weld line. Another microstructural characteristic was the occurrence of recrystallization within the weld zone of the linear friction welded IN 738. This microstructural feature along the weld line was previously observed in different Ni-based superalloys welded by frictional processes.[5,9,10] It was suggested that the recrystallization occurs dynamically due to the thermomechanical conditions imposed during friction welding, namely, the combination of high strain and strain rates at elevated temperatures. Figure 4 shows an optical micrograph of the recrystallized microstructure observed in the weld zone of IN 738. In particular, the maximum amount of plastic deformation would have occurred in the weld zone, which resulted in the formation of fine fully recrystallized grains. Traversing away from the weld line, the microstructure increasingly exhibited regions of deformed or partially recrystallized grains, such that beyond 300 μm the recrystallization was localized along prior grain boundaries. Overall, the observed marked changes in the microstructural characteristics (precipitates, carbides, and grain size) are related to the steep gradients in the temperature and deformation conditions within the weld zone.

The thermomechanically affected zone (TMAZ), region 2 in Figure 3, which is between 300 and 600 μm from the weld line, also exhibited a complete dissolution of the γ' precipitates and γ'-γ' eutectic, while the MC carbides remained. That is, the coarse and secondary γ' precipitates that were present in the preweld SHT IN 738 dissolved completely in both the weld zone and the TMAZ (600 μm from the weld line on either side of the joint). The main microstructural difference between the weld zone and the TMAZ is related to the recrystallization characteristics, in that fully recrystallized grains formed in the weld zone, while recrystallization in the TMAZ was localized to prior grain boundaries. In the HAZ, region 3 of Figure 3, secondary γ' precipitates that were produced by the preweld SHT dissolved completely, while the primary γ' precipitates dissolved partially, as revealed by the SEM micrograph of Figure 5. Region 3 differs from regions 1 and 2, in that only a partial dissolution of the coarse primary γ' precipitate was observed, which can be related to the temperature gradient that existed across the linear friction welded joint. No recrystallization was observed in the HAZ.

A significant microstructural change that is not usually reported to occur in linear friction welded materials is grain boundary liquation. Nevertheless, in this present study, intergranular and intragranular liquation were observed to have occurred in linear friction welded IN 738. Figure 6(a) is an SEM micrograph of the TMAZ showing evidence of grain boundary liquation in the welded material. Evidence of intragranular liquation is also provided by the SEM micrograph of Figure 6(b), which revealed the presence

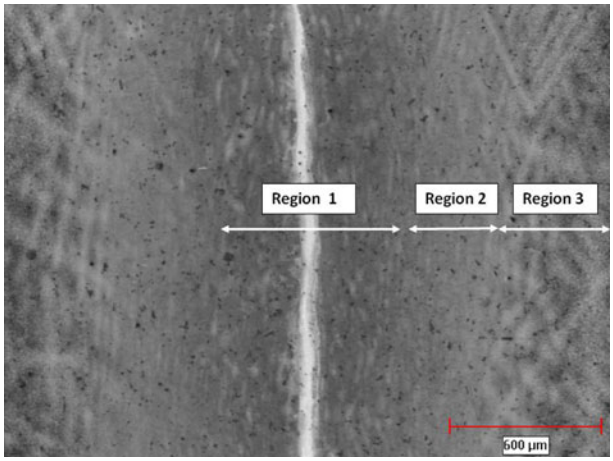

Fig. 3—Optical micrograph showing an overview of three regions characterizing the joint microstructure, namely, regions 1, 2, and 3, which correspond to the weld zone, the TMAZ, and the HAZ, respectively.

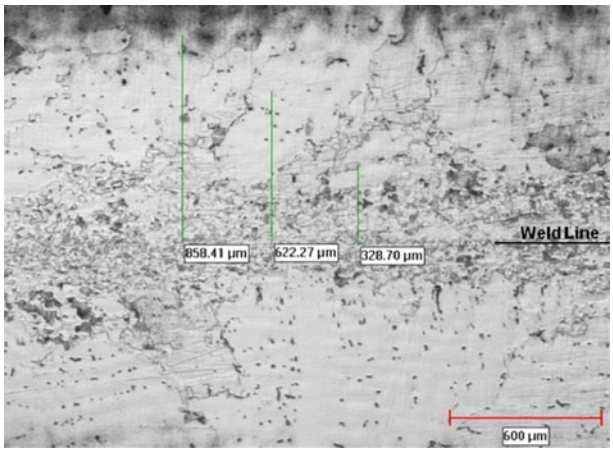

Fig. 4—Optical micrograph showing recrystallization across the weld joint.

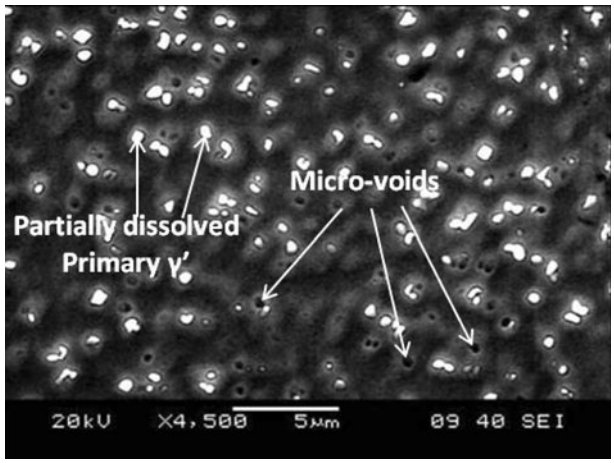

Fig. 5—SEM micrograph of HAZ.

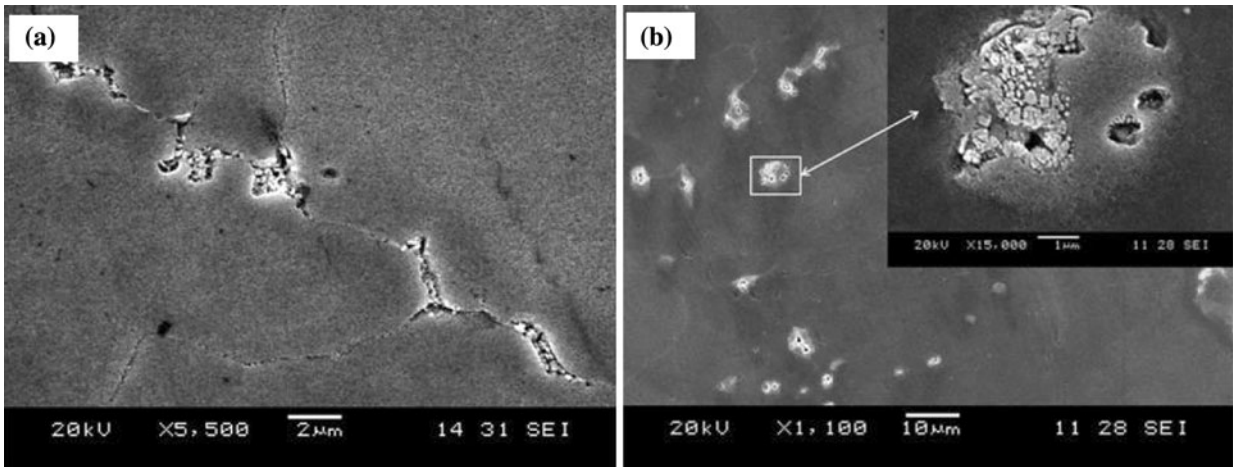

Fig. 6—SEM micrographs of the TMAZ showing (*a*) intergranular and (*b*) intragranular liquation.

of resolidified fine γ'-γ' eutectic products that formed from residual liquid during weld cooling. Evidence of intergranular or intragranular liquation was not found in the weld zone. The weld zone appeared essentially free from resolidified products and other microstructural features that indicate prior occurrence of liquation reaction. It is common knowledge that a temperature gradient exists across the linear friction welded joint with the highest temperatures existing in the weld zone. The temperature decreases with distance away from the weld line, into the TMAZ and the HAZ, and subsequently into the base material. The existence of a temperature gradient across the joint suggests that indications of liquation should be more evident in the weld zone in comparison to the TMAZ, which, however, was not the case. Apart from the effect of temperature on the microstructural changes that occurred in the welded material, another variable that was found to play a significant role in the observed microstructural development in this present work was the externally imposed compressive stress. Physical simulation of the welding process, using a Gleeble simulator, provided further insight into microstructural developments during linear friction welding of IN 738, as will be discussed subsequently.

C. *Gamma Prime (γ') Precipitate Dissolution Behavior*

Microstructural observations in this work suggest that a principal transformation that significantly influenced the microstructural response of IN 738 to the linear friction welding process, as has been generally recognized in other γ' strengthened nickel-based superalloys during friction joining,[10–13] is the dissolution of the strengthening γ' phase. In addition, γ' dissolution is generally used in theoretical models as an important parameter to predict maximum temperatures that different weld regions experience during friction welding.[12,14] However, there are two salient factors that are generally neglected in the application of these models, which, conceivably, could significantly affect the accuracy of the temperature predictions. First, an exclusive solid-state dissolution of γ' precipitates is normally assumed, which may cease to hold if the particles survive to temperatures where they could eutectically react with the surrounding matrix to produce a liquid phase. Second, a possible influence of the considerable magnitude of compressive stress, that induces compressive strain in the material being welded, on the degree of particle dissolution is not usually considered. These two factors are elucidated in Sections III–C–1 and III–C–2.

1. *Nonequilibrium dissolution of γ' precipitates during rapid thermal cycle*

The dissolution of γ' particles under an extremely slow heating rate, corresponding to an equilibrium condition, is expected to occur as the solubilities of their constituent elements in the matrix increase with increasing temperature such that the last remaining γ' particles will dissolve completely, by solid-state dissolution, at the equilibrium solvus temperature of the particles. However, the rapid thermal cycle usually experienced during friction welding departs significantly from equilibrium, with heating rates of the order of 473 K to 573 K (200 °C to 300 °C) per second and higher,[12] depending on the distance from the weld interface. It is known that the temperature of complete dissolution of second-phase particles increases with increasing heating rate and the extent of departure also depends on initial particle size.[12,15,16] Therefore, depending upon the initial particle size and heating rate, limited integrated time available for homogenization by the diffusion process during continuous heating can cause γ' precipitate particles in nickel-based superalloys to persist to temperatures well above their equilibrium solvus temperature. The γ' precipitates were generally reported to undergo solid-state dissolution during friction welding.[12] However, the survival of γ' precipitates to temperatures above their equilibrium solvus temperature, which occurs due to the rapid heating conditions during the contact phase of linear friction welding,[17] can lead to a nonequilibrium eutectic-type reaction between the precipitates and the γ-matrix to produce a metastable liquid through constitutional liquation phenomenon proposed by Pepe and Savage.[18] There exists a range of temperatures in γ' precipitation-hardened nickel-based alloys within which γ'-γ' eutectic reaction

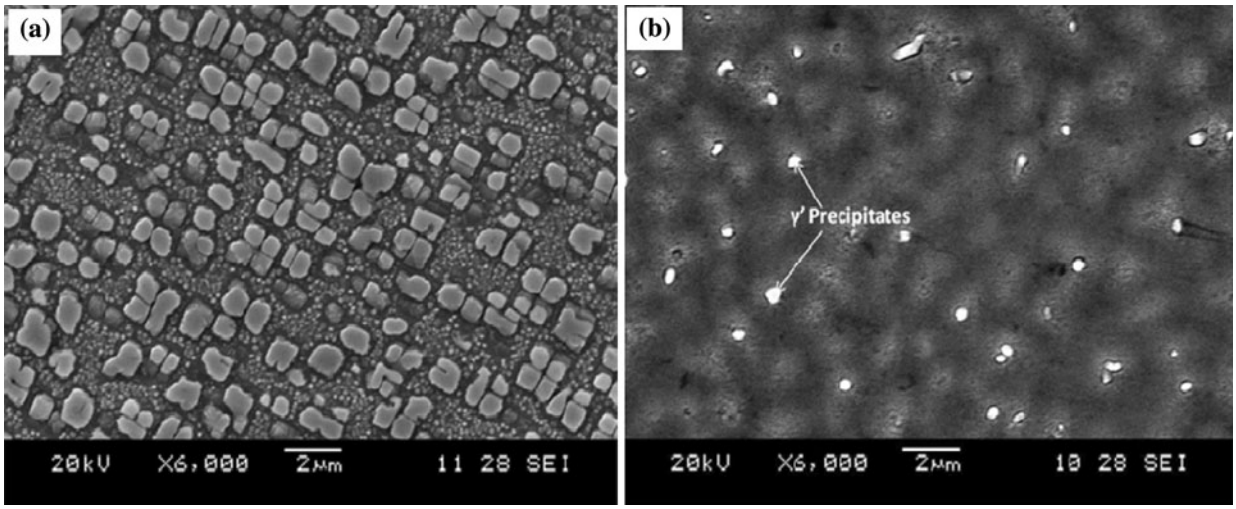

Fig. 7—(*a*) γ' precipitates in the SHT material and (*b*) γ' precipitate dissolution in a Gleeble-simulated material under rapid thermal cycle (heating rate of 150 °C/s) and 0.5 s holding time at the peak temperature of 1523 K (1250 °C).

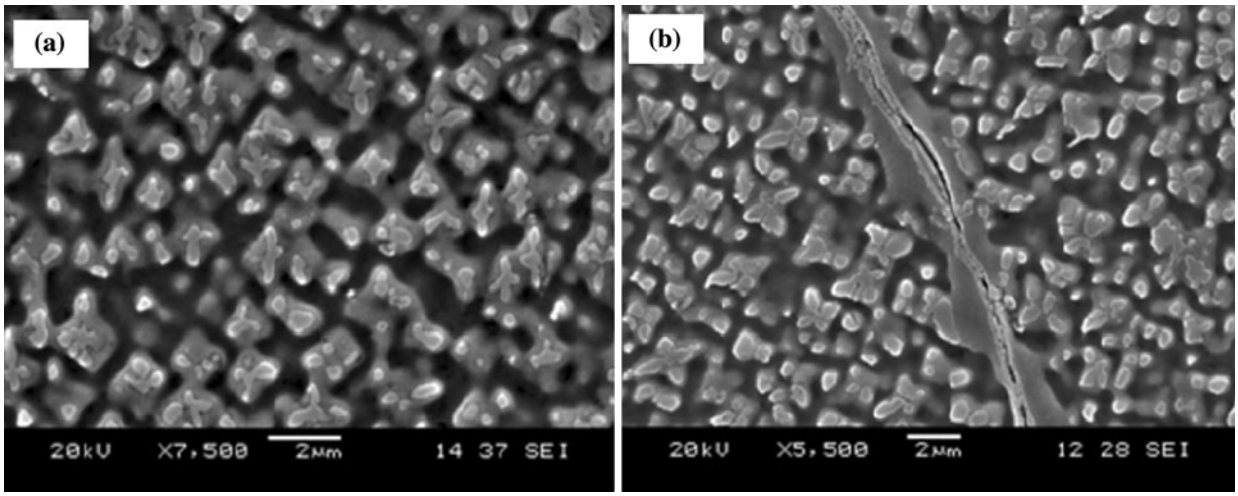

Fig. 8—Gleeble-simulated materials under rapid thermal cycle (heating rate of 150 °C/s) and 0.5 s holding time at peak temperatures of 1453 K (1180 °C), showing constitutional liquation of γ' precipitate and grain boundary liquation.

occurs, and the persistence of γ' particles to this temperature range during continuous heating could result in their constitutional liquation.[19] In IN 738, γ-γ' eutectic transformation was reported to occur over a range of temperatures, which could be below 1453 K (1180 °C).[20] In this present work, the results of Gleeble simulation of the welding thermal cycle showed that γ' particles survived well above their solvus temperature to peak temperatures of up to 1523 K (1250 °C) (Figure 7). This consequently resulted in their constitutional liquation. It is known that a differentially etching thin film connecting γ' particles is evidence of constitutional liquation.[19] SEM micrographs showing constitutionally liquated γ' particles in Gleeble-simulated IN 738 materials rapidly heated to 1453 K (1180 °C) are presented in Figures 8(a) and (b). Figure 8(b) shows that the constitutional liquation of γ' particles subsequently contributed to grain boundary liquation. Microstructural analysis of the linear friction welded IN 738 superalloy revealed that constitutional liquation of γ' precipitates occurred during joining (Figure 5). This is consistent with the observation of grain boundary and intragranular liquation in the welded material, as explained and presented earlier in Figures 6(a) and (b).

Aside from the thermal effects on γ' precipitate dissolution during linear friction welding, another factor that can significantly influence the degree to which the precipitates dissolved during joining is the imposed compressive stress that induces compressive strain in the material. Generally, the possible influence of compressive strain on the thermodynamics of precipitate dissolution during friction welding has received less attention and will be addressed next.

2. *Strain-assisted dissolution of γ' precipitates*

Previous reports on the microstructure of friction welded joints focused mainly on the effect of temperature on phase reactions. For example, in a model developed for the dissolution of γ' precipitates during

friction welding of a precipitation-hardened nickel-base superalloy, the solvus and the volume fraction of γ' precipitate were predicted on the basis of dissolution under thermal cycle alone.[12] Though the model was very useful in describing nonequilibrium dissolution behavior of the precipitates during rapid heating conditions, it did not consider the possibility of compressive strain aiding the dissolution kinetics of the precipitates. A generally accepted model for the dissolution of spherical second-phase particles in binary systems was developed by Whelan.[21] The model was used to evaluate the diffusion flux of solute out of a spherical precipitate of radius R. Whelan's model is given by[21]

$$\frac{dR}{dt} = -\frac{kD}{2R} - \frac{k}{2}\sqrt{\frac{D}{\pi t}} \qquad [1]$$

where D is the diffusivity of solute atoms in the matrix, t is the time taken, and k is given by[21]

$$k = \frac{2(\rho_s - \rho_e)}{(\rho_c - \rho_s)} \qquad [2]$$

where ρ_c is the solute concentration inside the precipitate, which is initially in equilibrium with a uniform concentration ρ_e of solute in the matrix, and ρ_s is the equilibrium surface concentration at time $t = 0$ when the temperature is raised by ΔT. According to Whelan,[21] the D/R term on the right-hand side of Eq. [1] arises from the steady-state part of the diffusion field, while the $t^{-1/2}$ term arises from the transient part. The model developed by Whelan (Eq. [1]) suggests that any factor that can increase the solute diffusivity, D, in the matrix will ultimately increase the dissolution rate.

The diffusivity, D, is temperature dependent, as given by the Arrhenius equation:

$$D = D_o \exp\left(\frac{-Q}{\mathrm{k}T}\right) \qquad [3]$$

where D_o is the pre-exponential factor, Q is the activation energy for diffusion, k is the gas constant, and T is the absolute temperature. Generally, more attention was given to the effect of temperature on the diffusion rate such that it is possible to erroneously assume that the activation energy for diffusion at a given temperature is constant. For the vacancy-assisted diffusion, Eq. [3] can be expanded to[22]

$$D = \frac{1}{6} d^2 Z v \exp\left[\frac{(\Delta S_f + \Delta S_m)}{\mathrm{k}}\right] \exp\left[\frac{-(\Delta H_f + \Delta H_m)}{\mathrm{kT}}\right] \qquad [4]$$

where d is the interatomic distance; Z is the coordination number; v is the vibrational frequency of an atom along its reaction path; ΔS_f and ΔS_m are the vacancy formation and migration entropies, respectively; and ΔH_f and ΔH_m are the vacancy formation and migration enthalpies, respectively. The first exponent and the parameters before it represent D_o in Eq. [3], while $(\Delta H_f + \Delta H_m)$ of the second exponent represents the activation energy, Q. The enthalpy change, ΔH, is dependent on both temperature and pressure. Consequently, the activation energy for diffusion, Q, at a given temperature, T, is dependent on pressure. The dependency of Q on pressure implies that the diffusivity, D, is dependent on pressure. Hence, it is conceivable that the kinetics of microstructural transformation in solids that are controlled by atomic diffusion can be affected by both the magnitude and sign of externally imposed stress/strain. Through a rigorous and meticulous analytical study, the following relationship between activation energy per unit strain, Q', and diffusion coefficients under strain, D (strain), and without strain, D (relax), was developed by Cowern *et al.*:[23]

$$D(\text{strain}) = D(\text{relax}) \exp\left(\frac{-Q's}{\mathrm{k}T}\right) \qquad [5]$$

where s is the strain (negative for compression and positive for tension), k is a constant, and T is the absolute temperature. It can be seen from this equation that atomic diffusion can be enhanced by compressive strain and reduced by tensile strain. This has been experimentally confirmed in SiGe material, where diffusion increased under compression but decreased under tension.[24] A similar variation in diffusion was also observed in a Cu-Si couple,[25] where the application of compressive stress resulted in a significant increase in diffusion.

In the present work, the dissolution of γ' precipitates, which is typically known to be controlled by diffusion of γ' forming elements away from the precipitate/matrix interface, was observed to be significantly enhanced by externally induced compressive strain. In the experiments performed to study the coupled effect of thermal cycle and externally imposed compressive stress on γ' precipitate dissolution in IN 738, two different temperature regimes were considered. In the first regime, the temperatures were below the equilibrium solvus temperature of the precipitates [about 1433 K (1160 °C)], where the precipitates are expected to dissolve by solid-state reaction, while the second regime was above the solvus temperature, where the precipitates are likely to dissolve by liquation reaction. Figures 9(a) and (b) show representative SEM micrographs of Gleeble-simulated specimens rapidly heated to 1383 K (1110 °C) and held for 20.5 seconds, followed by air cooling. The specimen in Figure 9(a) was subjected to the thermal cycle alone, while the specimen in Figure 9(b) was subjected to 20 pct compressive strain during holding at the peak temperature. As illustrated in Figures 9(a) and (b), the degree of precipitate dissolution in the stressed specimen (Figure 9(b)) was observed to be greater than that of the specimen subjected to thermal cycle alone (Figure 9(a)). Similar results were obtained for peak temperatures above 1383 K (1110 °C) but below the equilibrium solvus temperature of γ' precipitates.

Above the equilibrium solvus temperature of the precipitate, where γ' liquation was observed to occur, the degree of precipitate dissolution was also observed to be enhanced by compressive strain (Figures 10(a) and (b)). It is known that nonequilibrium intragranular liquid can isothermally resolidify through solid-state back-diffusion of solutes away from the liquid phase.[26]

The enhanced diffusivity of solute atoms in the matrix by an externally imposed compressive strain, as explained earlier, suggests an increased rate of back diffusion of solutes away from the liquid phase surrounding the precipitates into the adjacent γ matrix, resulting in a faster elimination of liquid produced by γ' liquation. Figures 10(a) and (b) are SEM micrographs of Gleeble-simulated specimens rapidly heated to 1443 K (1170 °C) and held for 1.5 seconds, followed by air cooling. The degree of precipitate dissolution in Figure 10(b), where 20 pct compressive strain was induced in the specimen at the peak temperature, was greater than that observed in

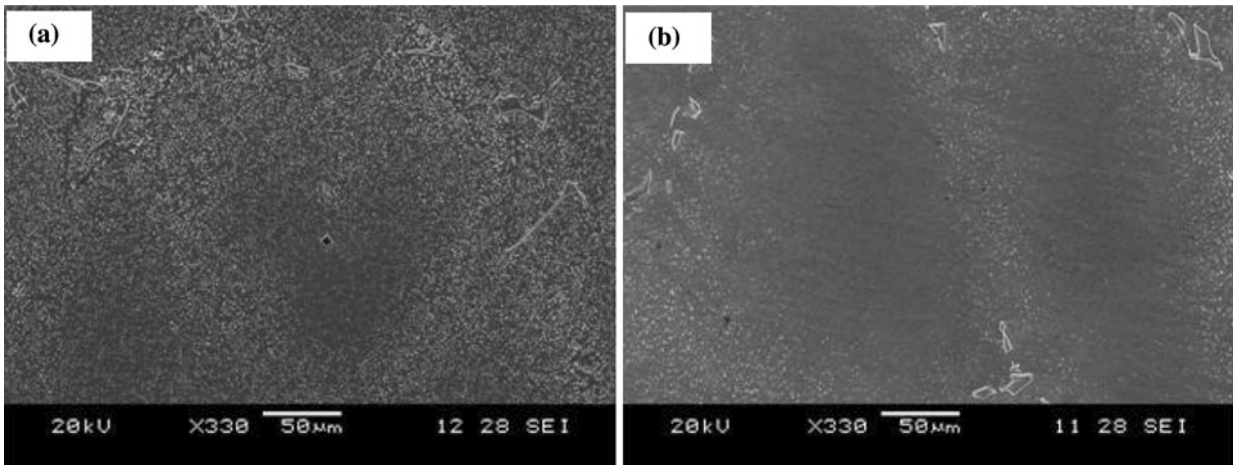

Fig. 9—Gleeble-simulated materials heated to 1383 K (1110 °C) peak temperature at 150 °C/s heating rate: (*a*) 20.5 s holding time without strain and (*b*) 20.5 s holding time with 20 pct strain, air-cooled.

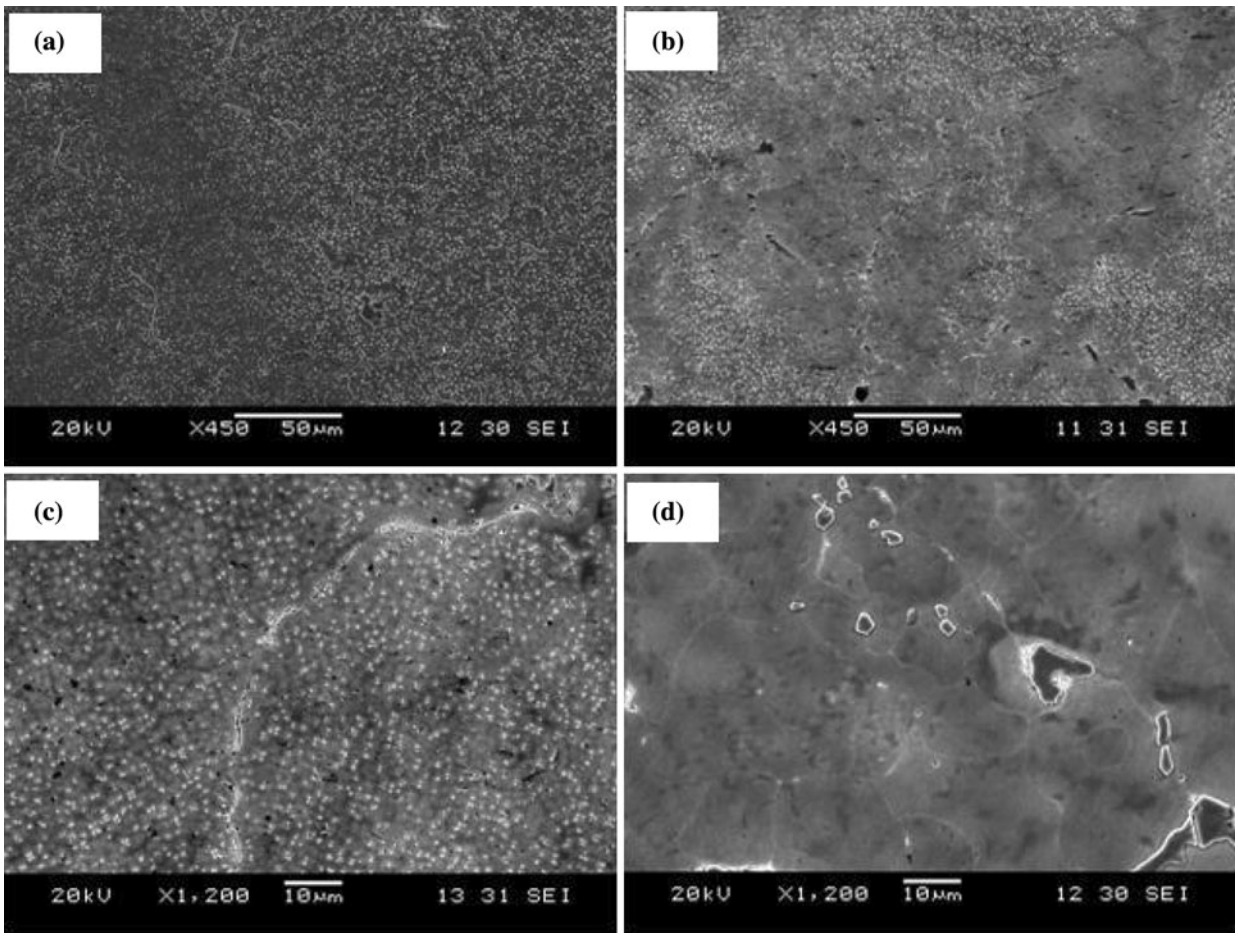

Fig. 10—Gleeble-simulated material heated to the peak temperature of 1443 K (1170 °C) at the rate of 150 °C/s: (*a*) 1.5 s holding time without strain, (*b*) 1.5 s holding time with 20 pct strain, (*c*) 3.5 s holding time without strain, and (*d*) 3.5 s holding time with 20 pct strain, air-cooled.

a specimen subjected to thermal cycle alone (Figure 10(a)). At an increased holding time (3.5 seconds) at the peak temperature of 1443 K (1170 °C), a region in the materials subjected to 20 pct compressive strain (Figure 10(d)) was almost completely devoid of γ' precipitates, while the precipitates only partially dissolved in the specimen subjected to thermal cycle alone (Figure 10(c)). Occurrences of strain-enhanced/induced dissolution of second-phase particles were also reported in other alloy systems.[27–30]

The possibility of strain-enhanced solute diffusivity and the concomitant strain-enhanced precipitate dissolution, as observed in this present work, suggest that the dissolution of γ' phase in nickel-based superalloys during linear friction welding can be significantly influenced by the compressive stress imposed on the material, especially during the forging stage of the process. As stated earlier, dissolution of γ' precipitates in nickel-based superalloys is commonly used in theoretical models to predict maximum temperature and associated mechanical properties in friction welded materials. The two main observations in this present work, *viz*. strain-enhanced dissolution and liquation reaction, can significantly increase the rate of dissolution of γ' particles such that the temperature of their complete dissolution may differ significantly from what is expected on the basis of exclusively solid-state dissolution mode. Hence, proper consideration of strain-enhanced dissolution and liquation reaction of γ' precipitates is paramount to the application of theoretical models to reliably predict the temperatures reached during linear friction welding and properties of the friction welded superalloys. Furthermore, these results establish that the formation of intergranular and intragranular liquid is possible during both conventional fusion welding and friction welding processes, fulfilling an important condition for intergranular liquation cracking in both processes. However, despite the occurrence of intergranular liquation during linear friction welding, grain boundary liquation cracking was not observed, as is usually the case during conventional fusion welding processes. Therefore, lack of cracking during friction welding is not due to lack of liquation, as is generally reported. In the present work, the important factors responsible for the preclusion of intergranular liquation cracking during linear friction welding will be discussed in Section III–2–D.

D. *Preclusion of Intergranular Liquation Cracking*

The presence of a liquid film along grain boundaries is a necessary, but not a sufficient, condition for intergranular liquation cracking, since cracking requires that on-cooling tensile stresses exceed the local strength at one of the solid-liquid interfaces to cause decohesion along the interface.[19] In other words, HAZ liquation cracking requires the coexistence of both liquated grain boundary and tensile stresses. The generation of tensile stress is critical for the liquation cracking to occur and must be present in the alloy at a temperature where continuous intergranular liquid film persists. The absence of cracking during linear friction welding, as observed in the present work, can be partly related to the state of stress within the workpiece during welding. Numerical simulation of the stress distribution in a material subjected to compressive axial loading, similar to that imposed during the forging stage of linear friction welding, has shown that most of the material is under compressive stresses, while tensile stress is mainly localized to regions extruded away from the joint area.[31] This suggests that imposing compressive load during the forging stage of linear friction welding can provide some resistance to crack formation. The counter-crack-formation effect of compressive loading is evident in a reported experimental work, where compressive stress did not only result in crack prevention but also caused healing of short cracks in nickel-base superalloy RENE88DT.†[32] Compressive stresses mainly dominate the joint area during the forging stage of the linear friction welding process, and the predominance of tensile stresses, which are usually later observed as residual stresses, occurs during continuous cooling after the forging stage. Therefore, despite the liquation of grain boundaries, application of compressive load during the forging stage appears to have contributed to preclusion of liquation cracking in the linear friction welded IN 738 by attenuating the driving force for cracking, which is the presence of tensile stresses during joining. This is supported by the presence of cracks observed in the extruded flash material (Figure 11), displaced from the joint area under the influence of the compressive force, where the state of stress is expected to be predominantly tensile in nature during joining. Tensile stresses are indeed generated during the friction welding process, as was reported.[33–35] Therefore, it is imperative to justify why the material did not crack despite the observed occurrence of liquation and the possibility of the presence of tensile stress.

†RENE88DT is a trademark of General Electric Company, Fairfield, CT.

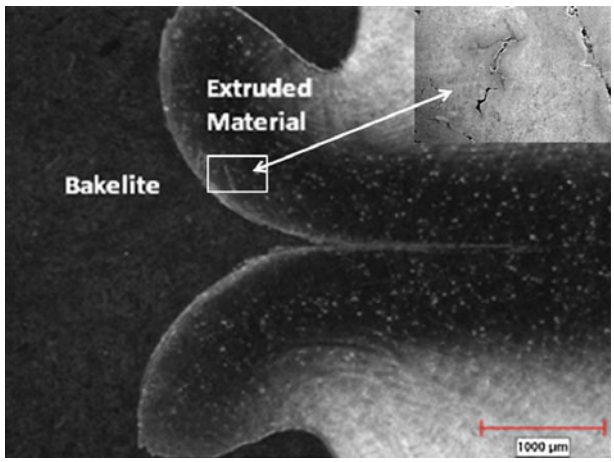

Fig. 11—Optical micrograph of the extruded flash material, with an inset showing cracks in the material where tensile stresses are present.

Intergranular liquation cracking during conventional fusion welding processes requires the stability of grain boundary liquid to lower temperatures at which tensile stresses generated during cooling could be sufficient to cause microfissuring by decohesion along one of the intergranular solid-liquid interfaces. Any factor that can reduce the stability of grain boundary liquid, such that the liquid does not persist to lower temperatures, will improve the material's resistance to weld liquation cracking. It was suggested that imposed strain on solids can thermodynamically drive a nonequilibrium system toward equilibrium.[36] The imposed compressive strain during linear friction welding has a tendency to reduce the stability of both intergranular and intragranular liquid produced during the welding process, by altering the kinetics of the resolidification process. The resolidification of metastable intergranular and intragranular liquid produced by the liquation of second-phase particles is diffusion dependent, and as discussed earlier, diffusion kinetics can be affected by both the magnitude and sign of externally imposed strain Eq. [5]. One method by which grain boundary liquid can resolidify is by solid-state back-diffusion of solute atoms away from the liquid phase into the solid matrix.[37] Intragranular liquid formed by the liquation of a second phase can also resolidify by solid-state back-diffusion, and at a rate determined by the solid-state diffusion.[26] Considering that solute diffusivity can be enhanced under compressive strain, even in superalloys, the effect of stress-induced compressive strain on back-diffusion controlled isothermal resolidification of intragranular metastable liquid was investigated in this work by Gleeble thermomechanical simulation. Intragranular liquid was produced by nonequilibrium eutectic-type transformation reaction between γ' precipitates and γ matrix by rapidly heating IN 738 superalloy to temperatures above the equilibrium γ' solvus temperature in the alloy [~1433 K (1160 °C)] up to 1503 K (1230 °C). It was observed, through the application of different levels of strain at various peak temperatures and holding times, that imposition of compressive strain significantly aided resolidification of the intragranular liquid. Figure 12(a) shows the microstructure of a Gleeble-simulated specimen rapidly heated to 1503 K (1230 °C), held for 2.5 seconds without strain, and air cooled. For comparison, Figure 12(b) shows the microstructure of a Gleeble specimen rapidly heated to 1503 K (1230 °C), held for 0.5 seconds, and then subjected to 25 pct compressive strain in 2 seconds followed by air cooling. Figure 12(a) is characterized by fine intragranular γ-γ' eutectic reaction products that formed from the liquid during cooling, indicating the stability of the liquid to lower temperatures where the resolidification products formed; whereas these features were completely eliminated under the influence of compressive strain, as shown in 12(b), indicating that complete rapid isothermal resolidification of the liquid took place at a higher temperature due to an enhanced back-diffusion. Similar observations were made when the holding time was increased. Figures 13(a) and (b) also show SEM micrographs of Gleeble-simulated materials at the same peak temperature of 1503 K (1230 °C) but a holding time of 10.5 seconds instead of 2.5 seconds, showing that the imposed strain was effective in rapidly resolidifying the liquid by enhanced back-diffusion. It should be added that significant intragranular liquation occurred at 1503 K (1230 °C) even after the 0.5-second holding time that was used prior to the application of stress, as presented in the SEM micrographs of Figures 14(a) and (b). The liquid formed by rapidly heating the alloy to 1503 K (1230 °C) persisted during the 2.5 and 10.5 seconds of holding under the application of thermal energy only and subsequently solidified at lower temperatures, during cooling, to produce the observed fine γ-γ' eutectic reaction products (Figures 12(a) and 13(a)). Nonequilibrium γ-γ' eutectic solidification is known to take place even when the temperature is as low as 1453 K (1180 °C) in alloy IN 738.[19] In contrast, however, the eutectic products were not observed in the specimen subjected to imposed stress-induced compressive strain (Figures 12(b) and 13(b)), which can be attributed to enhanced isothermal resolidification of the intragranular liquid during holding at the peak temperature, due to strain-aided solute back-diffusion. This observation of

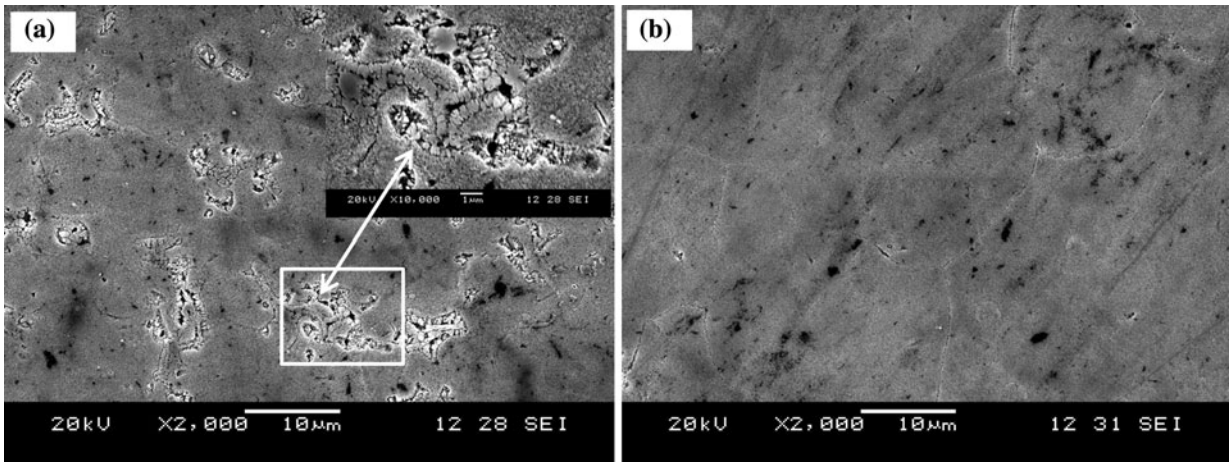

Fig. 12—SEM micrographs of Gleeble-simulated materials, showing (*a*) intragranular resolidified products at 1503 K (1230 °C) and (*b*) the absence of resolidified products at 1503 K (1230 °C) under strain.

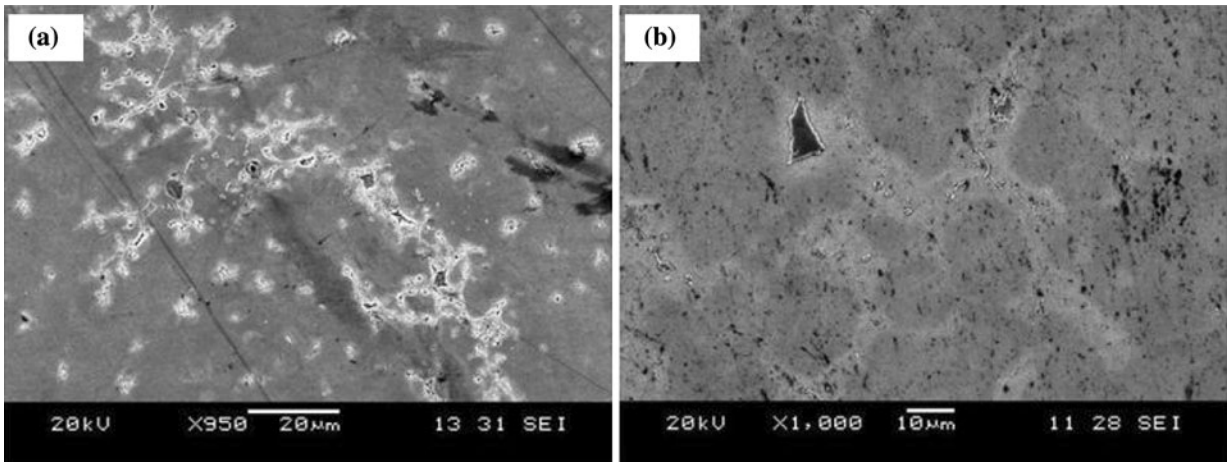

Fig. 13—Gleeble-simulated materials heated at 150 °C/s and held for 10.5 s at 1503 K (1230 °C) followed by air cooling, showing (*a*) intragranular resolidified products under thermal cycle alone and (*b*) the absence of resolidified products when 25 pct length reduction was imposed.

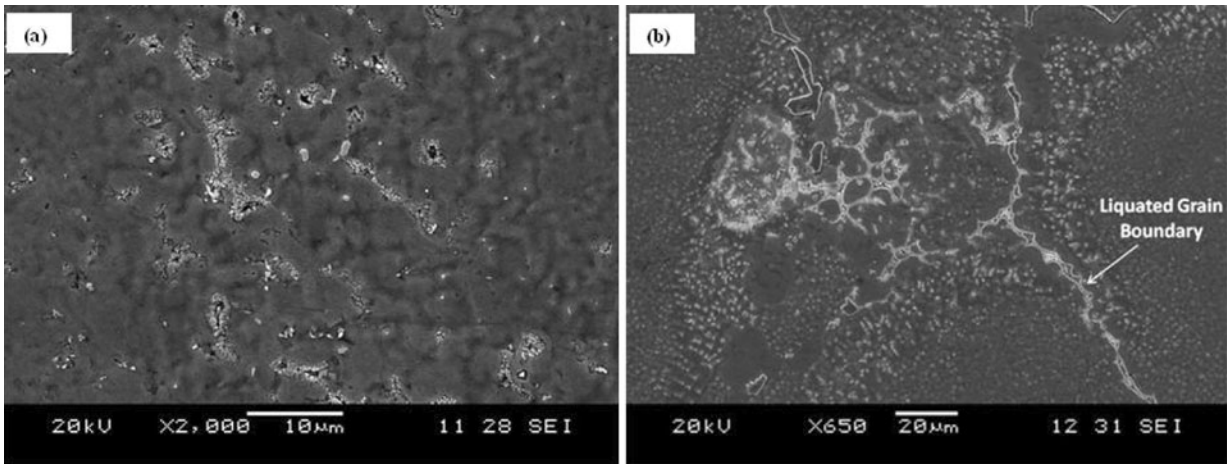

Fig. 14—Gleeble-simulated specimens heated at 150 °C/s to 1503 K (1230 °C), held for 0.5 s, and air-cooled, showing (*a*) intragranular resolidified products and (*b*) liquated eutectic area and liquated grain boundary.

strain-induced rapid back-diffusion is also supported by phase-field simulations by Li *et al.*,[38] where strain-induced increased diffusivity resulted in enhanced back-diffusion.

Aside from back-diffusion, another effective mode through which nonequilibrium grain boundary liquid can rapidly solidify at high temperatures is intergranular liquid film migration (LFM), which is characterized by a homogeneously alloyed solidified zone produced by the migration process of liquid films.[39] The most widely accepted mechanism that is used in explaining LFM is the diffusional coherency strain mechanism.[40] According to this, on introduction of a metastable liquid between two adjacent grains, a rapid equilibration process is set up by lattice solute back-diffusion. This results in composition-dependent variation in the lattice parameter between the solute-rich solid layer in contact with the liquid and the matrix well away from the solid-liquid interface. If there is a sufficient size difference between the solute and matrix atoms, coherency strains could develop within the grains due to the lattice mismatch. These strains would cause shifts in the free energy curve of the liquid-solid interface on either side of the film such that the compositions of the liquid and solid at equilibrium will be different at both solid-liquid interfaces. Ojo *et al.*[39] reported that atomic size mismatch between γ' forming elements and matrix atoms in IN 738 can induce intergranular LFM driven by diffusional coherency strain in the HAZ during conventional welding, where no externally applied stress is involved. During linear friction welding, however, imposed stress-induced compressive strain can significantly influence LFM by (1) aiding the initiation stage, (2) increasing the migration velocity, and (3) abetting the sustenance of the process, and these are discussed next.

In situations involving externally applied compressive stress, such as during linear friction welding, the initiation of LFM by generation of coherency strain, which is controlled by lattice solute back-diffusion, can be aided by strain-enhanced diffusivity. Furthermore, analytical modeling of the LFM process showed that the initial migration velocity, v, can be represented by the relationship[26]

$$v = \frac{D_L(\Delta C)}{(C_{L,T} - C_{S,T})\delta} \quad [6]$$

where D_L is the diffusivity in the liquid; δ is the initial liquid film thickness; ΔC is the concentration difference across the film; and $C_{L,T}$ and $C_{S,T}$ are the equilibrium concentrations of the solute(s) in the liquid and solid phases, respectively, at the solidifying interface. Fast solidification by the LFM process is dependent and controlled by rapid solute diffusional transport within the intergranular liquid film. The liquid state diffusion is primarily driven by the solute concentration gradient in the liquid, which is caused by a difference in composition of the liquid in contact with the two adjacent strained grains. The difference in the liquid composition, ΔC, arises due to the existence of a differential strain, $\Delta\varepsilon$, between the adjacent grains, which causes the liquid composition at equilibrium with the strained solids to differ. According to the diffusional coherency strain theory, despite an expected generation of similar levels of coherency stress in adjacent grains, owing to symmetrical lattice back-diffusion, $\Delta\varepsilon$ does exist between the grains. This is due to the difference in the values of the crystallographic orientation-dependent modulus of elasticity, Y, in the two grains.[41] An increase in $\Delta\varepsilon$ will produce a corresponding increase in ΔC, which would imply a higher driving force for LFM, and as such, any factor that effectively increases the magnitude of $\Delta\varepsilon$ can significantly accelerate the LFM process.

As discussed earlier, the diffusional coherency strain mechanism is used to explain LFM. However, the effect of externally applied stress on this mechanism is not usually considered. In this present work, the effect of externally applied compressive stress on the mechanism of LFM of metastable liquid is discussed. This is schematically illustrated in Figure 15. For a given set of Y values in two adjacent grains, the higher the magnitude of stress experienced by the grains, the higher will be $\Delta\varepsilon$. During conventional welding processes, where no externally applied stress is involved, based on the coherency strain mechanism, $\Delta\varepsilon$ is generated mainly by coherency strain produced by a change in the intragranular chemical composition induced by the solute lattice back-diffusion. However, during linear friction welding, in addition to diffusional coherency strain that may be present, an externally induced compressive strain, which is generally several orders of magnitude higher, is involved. The presence of a relatively large $\Delta\varepsilon$ owing to contributions from the externally applied stress could significantly alter the free energy curves of adjacent grains with respect to that of the liquid phase in between them, to produce a relatively high ΔC, as schematically illustrated in Figure 15. Ultimately, this would translate to a greater driving force and, concomitantly, a higher LFM velocity, based on Eq. [6], which would result in a larger migrated region relative to a situation under only imposed thermal environment. This factor was investigated in the present work by comparing the size of the LFM region in Gleeble-simulated specimens held for the same time period, with and without imposed stress. Figure 16(a) shows an SEM micrograph of a specimen simulated without imposed stress, while Figure 16(b) shows an SEM micrograph of a specimen simulated with imposed stress. The size of the migrated region in the specimen simulated under imposed stress (Figures 16(b)) was observed to be considerably larger (>100 pct) compared to that of the specimen simulated without externally applied stress (Figure 16(a)), which indicates a higher LFM velocity under stress.

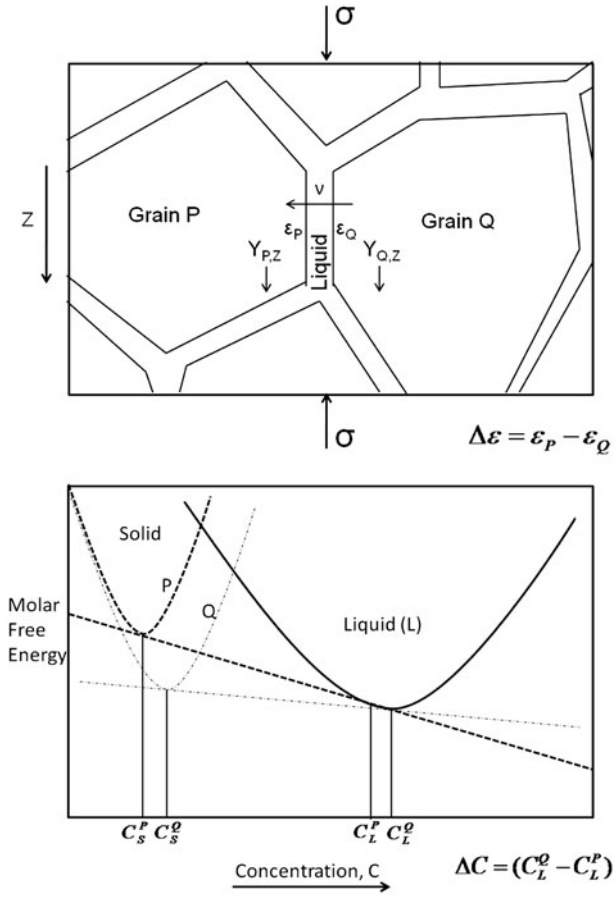

Fig. 15—Schematic diagram showing liquid film between two grains of different orientation-dependent elastic modulus, Y, and the corresponding free energy curves.

One major factor that limits the effectiveness of LFM is the significant reduction in its driving force, due to loss of coherency, which could result in immobility of grain boundary film, thus preventing complete elimination of the intergranular liquid. It has been recognized that the coherency strain energy is a function of the size of the migrated region,[42] and Baker and Purdy[26] suggested that coherency loss in the grain ahead of a migrating liquid film will occur when the effective solute penetration distance, D_s/v, becomes greater than or equal to the critical diffusion distance, L_s, required for the nucleation of misfit dislocation. In situations where an imposed stress is involved, such as during linear friction welding, the associated higher migration velocity, v, could significantly reduce D_s/v, such that the

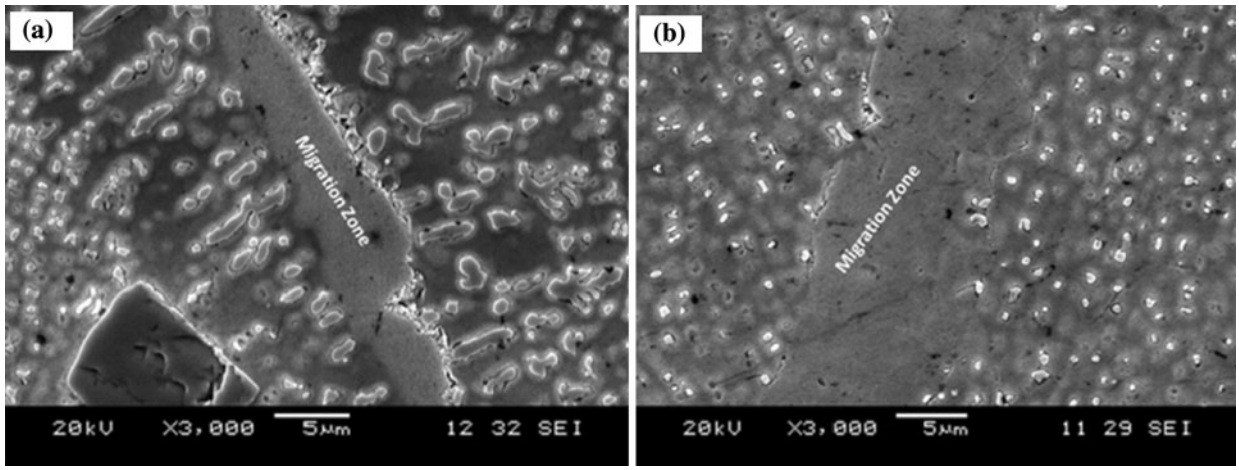

Fig. 16—LFM in Gleeble-simulated specimens heated at 150 °C/s and held at 1443 K (1170 °C) for 1.5 s, followed by air cooling (*a*) thermal environment alone and (*b*) thermal environment plus 20 pct strain at peak temperature.

condition of $D_s/v < L_s$ may persist for a longer time to sustain the process by coherency energy. Even in an eventual loss of coherency strain driving force, the $\Delta\varepsilon$ induced by the externally applied stress would serve as an extra source of driving energy to sustain rapid resolidification of the intergranular liquid through the LFM process. In addition, Brechet and Purdy[43] made an important comment on the LFM process, which is applicable to situations involving discrete liquating particles such as γ' precipitates in superalloys. They reported that a complete solidification of grain boundary liquid film would occur only under the non-steady-state migration process, in which the intergranular liquid is not being constantly supplied with extra solute atoms, such as from intragranular liquid. The enhanced resolidification of intragranular liquid under externally imposed stress-induced compressive strain, as observed in the present work, can shift the process toward such non-steady-state condition, where complete solidification of intergranular liquid by LFM is possible.

Microstructural studies of LFM regions in the present work showed that besides a smaller migrated region in the specimen simulated without imposed stress, nonequilibrium resolidified eutectic products formed ahead of the migrated zone, as shown in Figure 16(a). This implies that without the application of external stress, LFM was not effective in completely removing the grain boundary liquid during holding at the peak temperature, and the residual liquid ahead of the migrated zone transformed to eutectic products by nonequilibrium solidification reaction during cooling. A similar observation of ineffectiveness of LFM in completely removing intergranular liquid, due to a loss of driving energy, resulting in formation of eutectic products and the attendant microfissuring during conventional welding were previously reported by Ojo *et al.*[39] In contrast, resolidified eutectic products were not observed in the front of the migrated zone in Gleeble-simulated specimens subjected to an imposed compressive stress in the present work, as shown in Figure 16(b). This, in addition to a larger migrated zone, indicates that a more sustained LFM under imposed stress was effective in enabling a complete solidification of the intergranular liquid prior to cooling to lower temperatures, where the eutectic solidification reaction occurs. Therefore, imposed compressive stress enhanced the rapid high-temperature resolidification of intergranular liquid through LFM, which is characterized by a combination of enhanced initiation stage, higher migration velocity, and better sustenance. The elimination of both intergranular and intragranular liquid films during linear friction welding of IN 738 was achieved by a combination of solute back-diffusion and LFM, which were enhanced by imposed compressive strain. Therefore, contrary to the general conception, prevention of weld cracking during linear friction welding cannot be attributed to preclusion of liquation during joining; instead, rapid resolidification of intergranular and intragranular liquid aided by imposed compressive strain is a key factor that cannot be neglected in explaining the cracking resistance. Liquid films produced by constitutional liquation of γ' precipitates during rapid heating were effectively eliminated by the imposed stress such that the liquid films did not persist to lower temperatures during cooling.

The rapid resolidification processes, which seemed to have aided resistance to cracking, were enabled by the occurrence of plastic deformation. Therefore, the effectiveness of imposed compressive strain in aiding rapid solidification is made possible by the fact that a material containing grain boundary liquid can exhibit significant hot ductility under compression. This is in stark contrast to the case under tensile loading, where intergranular liquation produces zero hot ductility. It was suggested that, according to Gleeble hot ductility testing, a material loses all its ductility when the temperature reaches the on-heating nil-ductility temperature (NDT) and exhibits practically no ductility at all temperatures above the NDT. Investigations have shown that in a number of different materials, NDT occurs as a result of grain boundary liquation.[44] The temperature range between the liquidus T_L and the NDT represents the

on-heating zero ductility temperature range (ZDTR), within which the material exhibits practically zero ductility. The existence of tensile stresses in the material in this temperature range can result in cracking of the material. The results of Gleeble hot ductility testing performed on IN 738 by Ojo and Chaturvedi[19] revealed that the NDT of IN 738 was 1433 K (1160 °C). In this present work, the hot ductility behavior of IN 738 under imposed compressive stress contrasts the reported NDT behavior under tension. Gleeble thermomechanical simulations of the coupled rapid thermal cycle and imposed compressive stresses revealed that the hot ductility of the alloy was not zero under compression at temperatures in the on-heating ZDTR under tension. All Gleeble samples compressed at above the NDT exhibited appreciable amounts of plastic deformation despite the occurrence of constitutional liquation of γ' particles and subsequent observation of grain boundary liquation. This is in agreement with previous studies[45,46] on the deformation of semisolid materials where appreciably high amounts of deformation were experienced by the material under compression. Therefore, contrary to a condition where a material containing intergranular liquid undergoes intergranular cracking when subjected to tensile loading, a material containing intergranular liquid exhibits hot ductility under compressive loading, thereby aiding rapid resolidification of the liquid and subsequent enhanced resistance to cracking.

Rapid resolidification of intergranular and intragranular liquid aided by stress-induced compressive strain, as observed in this work, is a key factor that cannot be neglected in the understanding of cracking resistance. Another major finding in the present study was that it is not only the cracking resistance that can be adequately understood by studying the effect of compressive strain; in fact, microstructural changes induced in the material during joining cannot be properly understood without a careful analysis of the coupled thermal and strain effects. One major constraint to the full understanding of weld zone microstructure in materials joined by frictional processes is the measurement of the actual temperature reached at the weld interface. The knowledge of the actual peak temperature at the weld interface can aid the understanding of microstructural development during joining, and this will be discussed in Section III–E.

E. *Peak Temperature in the Weld Zone*

Efforts have been made to evaluate the peak temperatures reached in friction welds by the use of thermocouples.[6,47] Though thermocouples make contact with the material at the point where the measurements were made, and their results are often generally acceptable, they are limited in that they can only measure temperatures at distances away from the weld line such that the actual temperature at the weld interface is difficult to determine. Another method involves the use of microstructural study to estimate the peak temperature attained during friction welding.[12,14] In this work, an attempt was made to evaluate the peak temperature reached at the weld interface during linear friction welding of IN 738 by using a microstructural examination approach. This was achieved by a careful correlation of weld microstructures with those of Gleeble thermomechanically simulated materials at different temperatures and different amounts of induced compressive strains. As discussed earlier, intragranular resolidified γ-γ' eutectic products were observed in the TMAZ in the welded specimen. During Gleeble simulation, these intragranular eutectic products were only observed in specimens simulated at 1503 K (1230 °C) and above. Figures 17(a) and (b) are SEM micrographs of Gleeble materials rapidly heated to 1473 K (1200 °C) and held for 3.5 and 10.5 seconds, respectively. These show that the grain interiors were essentially free from these resolidified products, even after holding for over 10 seconds. On increasing the temperature to 1503 K (1230 °C), intragranular resolidified eutectic products were observed even after a short holding time of 2.5 seconds. This finding suggests that the temperature in the TMAZ, where intragranular resolidified eutectic products were observed, was not below 1503 K (1230 °C). Since the temperature would have been greatest in the weld zone, compared to TMAZ and

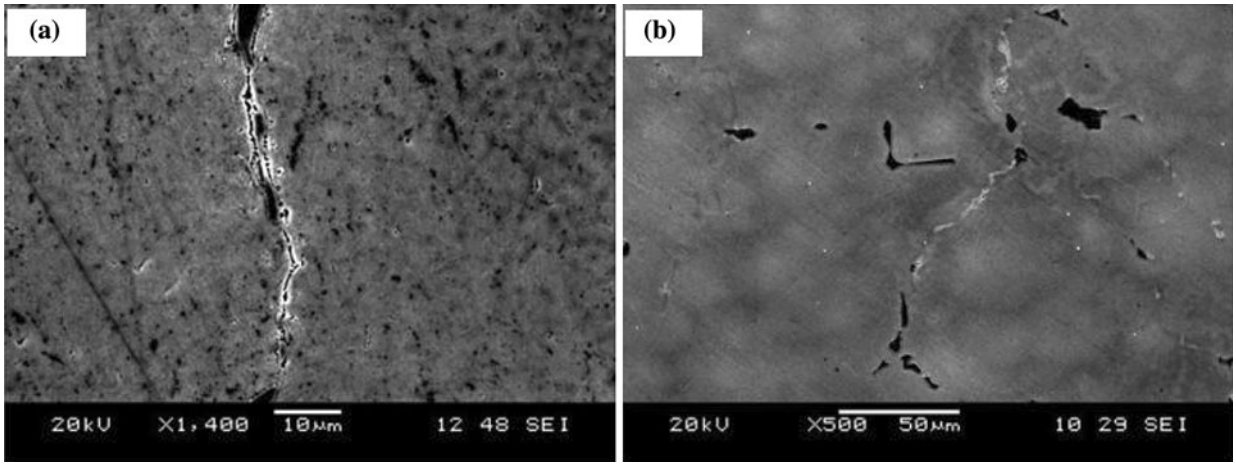

Fig. 17—Gleeble-simulated materials heated at 150 °C/s to the peak temperature of 1473 K (1200 °C) and held for (*a*) 3.5 s and (*b*) 10.5 s, followed by air cooling.

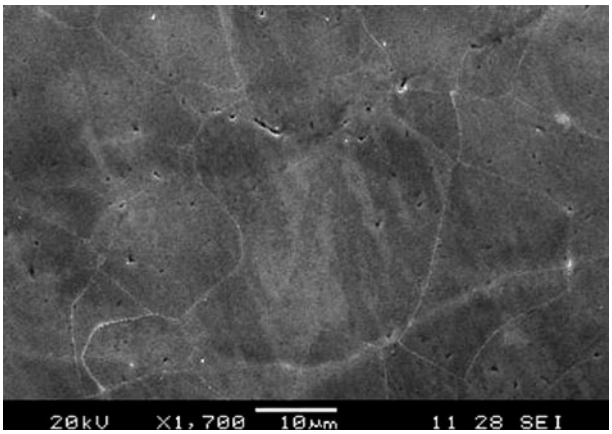

Fig. 18—Weld zone microstructure, adjacent to the weld line.

HAZ, the peak temperature reached in the weld zone during linear friction welding of IN 738 was likely to be more than 1503 K (1230 °C). This is in agreement with a recently reported study that showed that the peak temperature within the weld zone during friction processing of a material can be up to 0.9 to 0.97 T_m, where T_m is the melting temperature.[48] In addition, pyrometer measurements during friction welding of a nickel-based superalloy, ASTROLOY,‡ reportedly showed that the weld zone temperature was up to 1553 K (1280 °C).[12]

‡ASTROLOY is a trademark of General Electric Company, Fairfield, CT.

Notably, the weld zone microstructure in the linear friction welded IN 738, as presented in Figure 18, is not consistent with what is expected at high temperatures (such as 1503 K (1230 °C) and above) on an exclusive basis of the thermal effect. The formation of this type of microstructure cannot be duly explained without considering and incorporating the phenomenon of strain-induced rapid solidification that was observed in this work. As stated earlier, rapid heating of IN 738 to 1453 K (1180 °C) and above produces intergranular and intragranular liquation with resultant as-cooled microstructure consisting of resolidified eutectic products. Nevertheless, such resolidified eutectic products were not observed within the weld zone of the linear friction welded specimen despite indications that the peak temperature that was reached there during joining was, at least, 1503 K (1230 °C). This can be attributed to rapid resolidification of nonequilibrium liquid produced on heating to the peak temperature, facilitated by the considerable compressive strain experienced by the weld zone during welding. The TMAZ (away from the weld interface), which experienced marginal strain compared to the weld zone, contained the resolidified eutectic products (Figure 6(b)). This is at variance with what is typically observed in conventionally welded materials, in that formation of resolidified eutectic products normally increases toward the weld zone and is often accompanied by liquation cracking. The disparity can be explained by the absence of an externally applied stress during conventional welding, which is present during linear friction welding.

F. *OIM Study of Recrystallized Grains*

The EBSD based OIM analysis revealed that the average diameter of the recrystallized grains in the weld zone was about 13.9 μm. Most of the recrystallized grain boundaries had Σ values greater than 29, implying a very high degree of disorder. Figures 19(a) and (b) show the unique grains formed on both sides of the weld centerline and the character of the grain boundaries, respectively, with black lines representing grain boundaries of $\Sigma > 29$. An OIM image (Figure 20(a)) of a region of transition from the weld zone to the TMAZ (about 300 μm from the weld line) confirmed an earlier suggestion that the TMAZ exhibited partial recrystallization such that recrystallization became mainly localized on prior grain boundaries. The character of the grains at the transition region is also presented in the OIM image of Figure 20(b).

A notable observation about the recrystallization behavior in the weld zone of linear friction welded IN 738 was the presence of finer (smaller) grains at the weld centerline area (Figures 19(a) and (b)) compared to other weld zone areas away from the centerline. In the weld zone, complete recrystallization of the grains was observed at both the weld centerline and adjacent weld zone areas. It is known that there is a temperature range, ΔT, within which recrystallization and grain growth occur, and following complete recrystallization, a combination of high temperature and longer holding time within the ΔT normally aids the growth of newly formed fine grains to produce grains of larger size. The weld centerline area experienced the highest peak temperature during joining. Also, the joint area cools by the conduction of heat away from regions of higher temperature to regions of lower temperature in the base material. It is, therefore, reasonable to conceive that the weld centerline area, which experienced the highest temperature, spent a longer time within ΔT, compared to other weld zone areas. Consequently, larger grain size is expected at the weld centerline area of the weld zone due to the fact that it experienced the highest temperature and longest time within ΔT. The formation of grains of larger sizes at the weld centerline, compared to other weld zone areas, of friction welded materials were reported in the literature.[5,10] However, the observation of smaller grains at the weld centerline area relative to other weld zone areas in this present work is in contrast to the normally expected larger grains, which suggests that weld microstructure may not be solely explainable by classical solid-state recrystallization theory. The observed deviation from the expected behavior can be related to the liquation-resolidification processes that took place during joining. As previously stated, liquation occurred in these regions during joining. Since recrystallization is generally known to be a solid-state phenomenon, it is conceivable that recrystallization in the liquated regions would have occurred after complete solidification of the metastable liquid produced in these regions during the joining process. This implies that

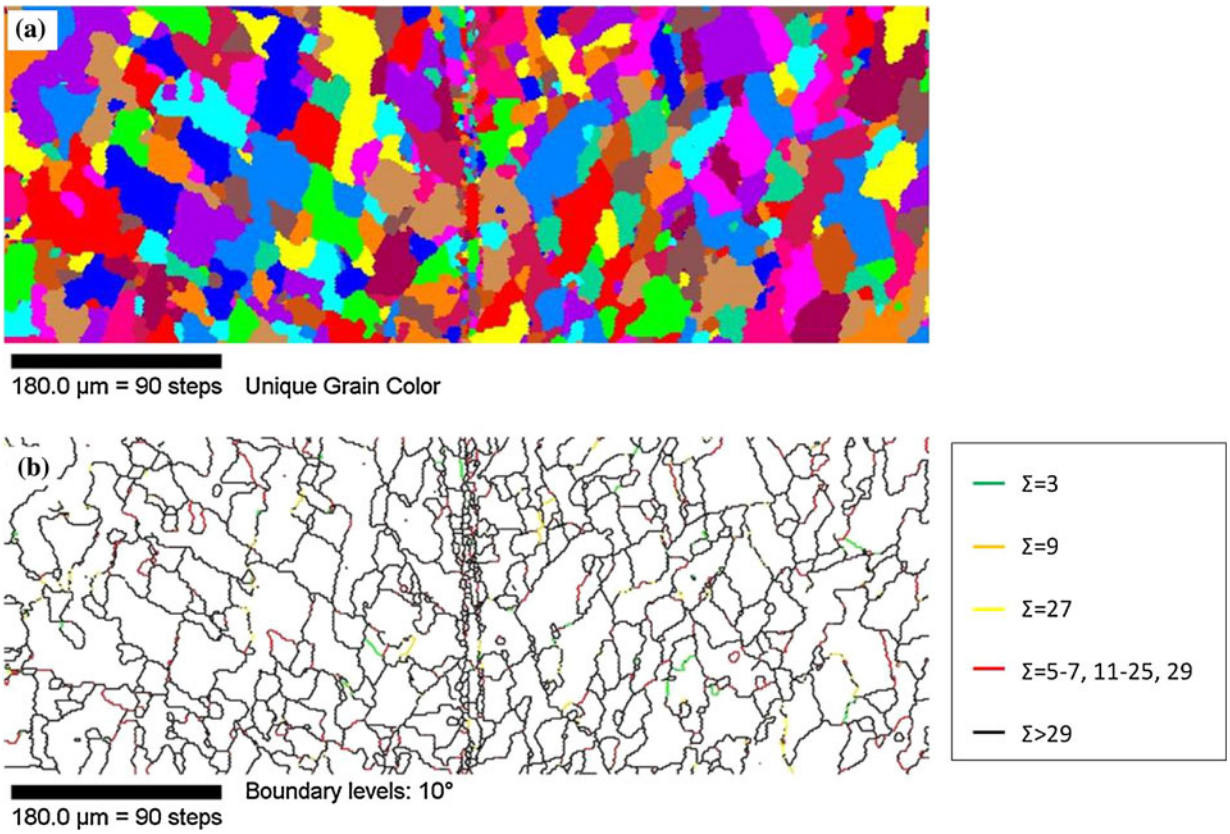

Fig. 19—OIM images showing (*a*) the unique recrystallized grains across the weld centerline and (*b*) the character (Σ values) of boundaries between the recrystallized grains.

recrystallization may provide some information about the resolidification behavior in the material. In the region that solidified last, possibly due to the presence of more liquid, recrystallization might have commenced later compared to those regions that solidified earlier due to a relatively smaller amount of liquid. In such a situation, recrystallized grains in the weld centerline area can be smaller than those in other regions. Gleeble simulations showed that the extent of liquation increased with temperature. This implies that the highest amount of liquation would have occurred at the weld centerline area, due to this region being at the highest peak temperature, and this weld centerline area could have solidified last compared to other areas in the weld zone. Hence, recrystallization could have started later at the weld centerline area and, thus, will have finer grains relative to other regions, as observed by OIM. This observation, which does not seem to be explainable exclusively by solid-state reaction, is consistent with the concepts of nonequilibrium liquation reaction and strain-induced rapid solidification during linear friction welding, as reported and discussed in this work.

IV. SUMMARY AND CONCLUSIONS

1. Linear friction welding produced a sound and crack-free joint in IN 738, an alloy generally considered to be very difficult to weld due to its high susceptibility to HAZ liquation cracking during welding.
2. Linear friction welding of IN 738 was accompanied by significant microstructural changes across the joint, including complete dissolution of the main strengthening, γ', phase within about 600 μm on either side of the weld line.
3. The study revealed that, during the forging stage of the welding process, the application of externally imposed compressive stress can significantly aid the rate of dissolution of γ' precipitates.
4. In variance to the generally held views and reports, grain boundary liquation occurred during linear friction welding of IN 738 as a result of nonequilibrium phase reaction between γ' particles and the surrounding γ matrix.
5. Occurrence of intergranular liquation did not result in liquation cracking, as is the usual case during conventional fusion welding processes. Therefore, contrary to the general conception, prevention of weld cracking during the process is not due to preclusion of liquation during joining.
6. Resistance to cracking can be attributed to the counter-crack-formation effect of the compressive stress imposed on the material during forging and a rapid resolidification of intergranular and intragranular liquid aided by the induced compressive strain.
7. The result of this work indicates that the peak temperature reached in the weld zone during linear friction welding of IN 738 was likely to be greater than 1503 K (1230 °C).

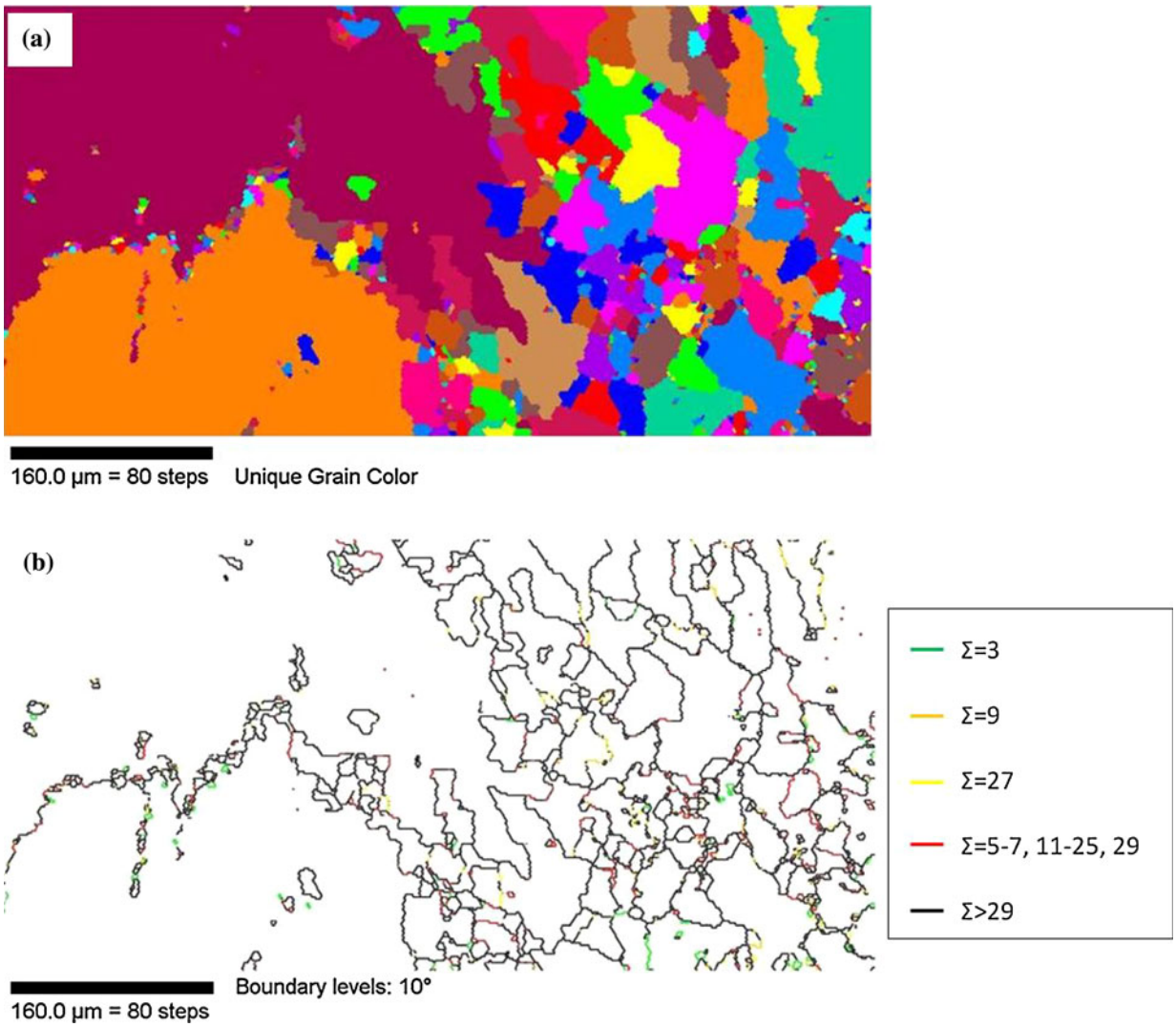

Fig. 20—OIM images showing (*a*) the unique recrystallized grains at the transition region between the weld zone and TMAZ, and (*b*) the character (Σ values) of boundaries between the recrystallized grains at the transition region.

8. Complete recrystallization occurred in the weld zone of the welded material. Two regions could be identified in the weld zone: the weld centerline area, where finer grains formed; and the other weld zone areas, where the recrystallized grains were of larger size. The formation of finer recrystallized grains at the weld centerline area, relative to other weld zone areas, is consistent with the concepts of nonequilibrium liquation reaction and strain-induced rapid solidification.
9. Besides resistance to cracking, nonequilibrium liquation reaction and strain-induced rapid solidification discussed in this work are pertinent to the understanding of the microstructure developed in the welded material.

ACKNOWLEDGMENTS

The authors acknowledge the financial support received from NSERC. The technical assistance of M. Guérin and E. Dalgaard for linear friction welding of IN 738 is greatly appreciated. O.T. Ola is also grateful to the University of Manitoba for the award of a Graduate Fellowship.

REFERENCES

1. M. Prager and C.S. Shira: *Weld. Res. Council Bull.*, 1968, vol. 128, pp. 1–55.
2. O.A. Ojo, N.L. Richards, and M.C. Chaturvedi: *Mater. Sci. Technol.*, 2004, vol. 20, pp. 1027–34.
3. O.A. Ojo, N.L. Richards, and M.C. Chaturvedi: *Metall. Mater. Trans. A*, 2006, vol. 37A, pp. 421–33.
4. A.T. Egbewande, H.R. Zhang, R.K. Sidhu, and O.A. Ojo: *Metall. Mater. Trans. A*, 2009, vol. 40A, pp. 1694–2704.
5. C. Mary and M. Jahazi: *Adv. Eng. Mater.*, 2008, vol. 10, pp. 573–78.
6. A. Vairis and M. Fros: *Wear*, 1998, vol. 217, pp. 117–31.
7. M. Karadge, M. Preuss, P.J. Withers, and S. Bray: *Mater. Sci. Eng. A*, 2008, vol. 491, pp. 446–53.
8. A.N. Davies: *Exploiting Friction Welding in Production*, The Welding Institute, Cambridge, United Kingdom, 1979, pp. 20–29.

9. S. Vardhan Lalam, G. Madhusudhan Reddy, T. Mohandas, M. Kamaraj, and B.S. Murty: *Mater. Sci. Technol.,* 2009, vol. 25, pp. 851–61.
10. M. Preuss, J.W.L. Pang, P.J. Withers, and G.J. Baxter: *Metall. Mater. Trans. A*, 2002, vol. 33A, pp. 3215–25.
11. F. Daus, H.Y. Li, G. Baxter, S. Bray, and P. Bowen: *Mater. Sci. Technol.*, 2007, vol. 23, pp. 1424–32.
12. M. Soucail and Y. Bienvenu: *Mater. Sci. Eng. A*, 1996, vol. 220, pp. 215–22.
13. O.M. Barabash, R.I. Barabash, G.E. Ice, Z. Feng, and D. Gandy: *Mater. Sci. Eng. A*, 2009, vol. 524, pp. 10–19.
14. M. Soucail, A. Moal, L. Naze, E. Massoni, C. Levaillant, and Y. Bienvenu: *Superalloys 1992*, TMS, Warrendale, PA, 1992, pp. 847–56.
15. B.I. Bjorneklett, O. Grong, O.R. Myhr, and A.O. Kluken: *Acta Mater.*, 1998, vol. 46, pp. 6257–66.
16. D.L. Sponseller: *Superalloys Conf.*, TMS, Champion, PA, 1996, pp. 259–70.
17. E. Dalgaard, P. Wanjara, X. Cao, J. Gholipour, and J.J. Jonas: *Aerospace Materials & Manufacturing: Advances in Materials, Processes and Repair Technologies*, 49th Annual Conf. of Metallurgists (COM2010, Vancouver), CIM, Montreal, 2010, pp. 69–78.
18. J.J. Pepe and W.F. Savage: *Weld. J.*, 1967, vol. 46, pp. 411s–422s.
19. O.A. Ojo and M.C. Chaturvedi: *Mater. Sci. Eng. A*, 2005, vol. 403, pp. 77–86.
20. R. Rosenthal and D.R.F. West: *Mater. Sci. Technol.*, 1999, vol. 15, pp. 1387–94.
21. M.J. Whelan: *Met. Sci. J.*, 1969, vol. 3, pp. 95–97.
22. A.K. Jena and M.C. Chaturvedi: in *Phase Transformation in Materials*, Brendan M. Stewart, ed., Prentice-Hall Inc., Englewood Cliffs, NJ, 1992, pp. 66–131.
23. N.E.B. Cowern, P.C. Zalm, P. Van der Sluis, D.J. Gravensteijn, and W.B. de Boer: *Phys. Rev. Lett*, 1994, vol. 72, pp. 2585–88.
24. P. Kringhøj, A.N. Larsen, and S.Y. Shirayev: *Phys. Rev. Lett.*, 1996, vol. 76, pp. 3372–75.
25. M. Onishi and H. Miura: *Trans. JIM*, 1977, vol. 18, pp. 107–12.
26. S.W. Baker and G.R. Purdy: *Acta Mater.*, 1998, vol. 46, pp. 511–24.
27. E. Nes: *Met. Sci.*, 1979, vol. 13 (3–4), pp. 211–15.
28. C.R. Hutchinson, P.T. Loo, T.J. Bastow, A.J. Hill, and J. da Costa Teixeira: *Acta Mater*, 2009, vol. 57, pp. 5645–53.
29. V.V. Sagaradze, V.A. Shabashov, T.M. Lapina, N.L. Pecherkina, and V.P. Pilyugin: *Phys. Met. Metallogr.*, 1994, vol. 78 (6), pp. 619–28.
30. Y. Ivanisenko: *Mater. Sci. Forum,* 2007, vols. 539–543, pp. 4681–86.
31. F. Ju, Z. Xa, B.J. Diak, O.A. Ojo, W.D. MacDonald, and M. Niewczas: *Magnesium Science and Technology—Automotive Lightweighting*, Detroit, MI, Apr. 14–17, 2008.
32. X. Zhao, X. Lin, J. Chen, L. Xue, and W. Huang: *Mater. Sci. Eng. A*, 2009, vol. 504, pp. 129–34.
33. Y.-C. Kim and A. Fuji: *Sci. Technol. Weld. Join.*, 2002, vol. 7 (3), pp. 149–54.
34. M. Preuss, P.J. Wither, and G.J. Baxter: *Mater. Sci. Eng., A*, 2006, vol. 437, pp. 38–45.
35. M. Karadge, P. Frankel, A Steuwer, C. Lovell, S. Bray, P.J. Withers, and M. Preuss: *Joining of Advanced and Specialty Materials*, Materials Science and Technology (MS&T), 2006: Product Manufacturing, pp. 35–44.
36. J.D. Embury, A. Deschamps, and Y. Brechet: *Scripta Mater.*, 2003, vol. 49, pp. 927–32.
37. B. Radhakrishnan and R.G. Thompson: *Metall. Mater. Trans. A*, 1992, vol. 23A, pp. 1783–98.
38. J. Li, J. Wang, and G. Yang: *J. Cryst. Growth*, 2009, vol. 311, pp. 1217–22.
39. O.A. Ojo, N.L. Richards, and M.C. Chaturvedi: *Scripta Mater.*, 2004, vol. 51, pp. 141–46.
40. M. Hillert: *Scripta Metall.*, 1983, vol. 17, pp. 237–40.
41. C.A. Handwerker, J.W. Cahn, D.N. Yoon, and J.E. Blendell: in *Diffusion in Solids: Recent Developments*, M.A. Dayananda and G.E. Murch, eds., TMS, Warrendale, PA, 1985, pp. 275–92.
42. J.W. Matthews: in *Dislocations in Solids*, F.R.N. Nabarro, ed., North Holland, Amsterdam, 1979, vol. 2.
43. Y. Brechet and G.R. Purdy: *Scripta Metall.*, 1988, vol. 22, pp. 1629–33.
44. W. Lin, J.C. Lippold, and W.A. Baeslack, III: *Weld J.*, 1993, vol. 72, pp. 135s–153s.
45. Y. Lu, M. Li, W. Huang, and H. Jiang: *Mater. Character.*, 2005, vol. 54, pp. 423–30.
46. D. Zhang, B. Yang, J. Zhang, Y. Zhang, and B. Xiong: *Trans. Nonferrous Met. Soc. China*, 2005, vol. 15, pp. 1125–29.
47. C. Mary and M. Jahazi: *Adv. Mater. Res.*, 2006, vols. 15–17, p. 357.
48. S. Swaminathan, K. Oh-Ishi, A.P. Zhilyaev, C.B. Fuller, B. London, M.W. Mahoney, and T.R. Mcnelley: *Metall. Mater. Trans. A*, 2010, vol. 41A, pp. 631–40.